

Electronic Supplementary Information on:

Reduced Graphene Oxide-Nickel
Nanoparticles/Biopolymer Composite Films for Sub-
Millimolar Detection of Glucose

Rahul Krishna,^{1,2,3} José M. Campiña,^{1*} Paula M. V. Fernandes,¹ João Ventura,³ Elby
Titus,² António F. Silva¹

¹ Centre for Research in Chemistry of the University of Porto (CIQUP), Dept. of Chemistry and Biochemistry, Faculty of Sciences, Rua do Campo Alegre, s/n, 4169-007, Porto, Portugal.

² Centre for Mechanical Technology and Automation (TEMA), Dept. of Mechanical Engineering, University of Aveiro, 3810-193, Aveiro, Portugal.

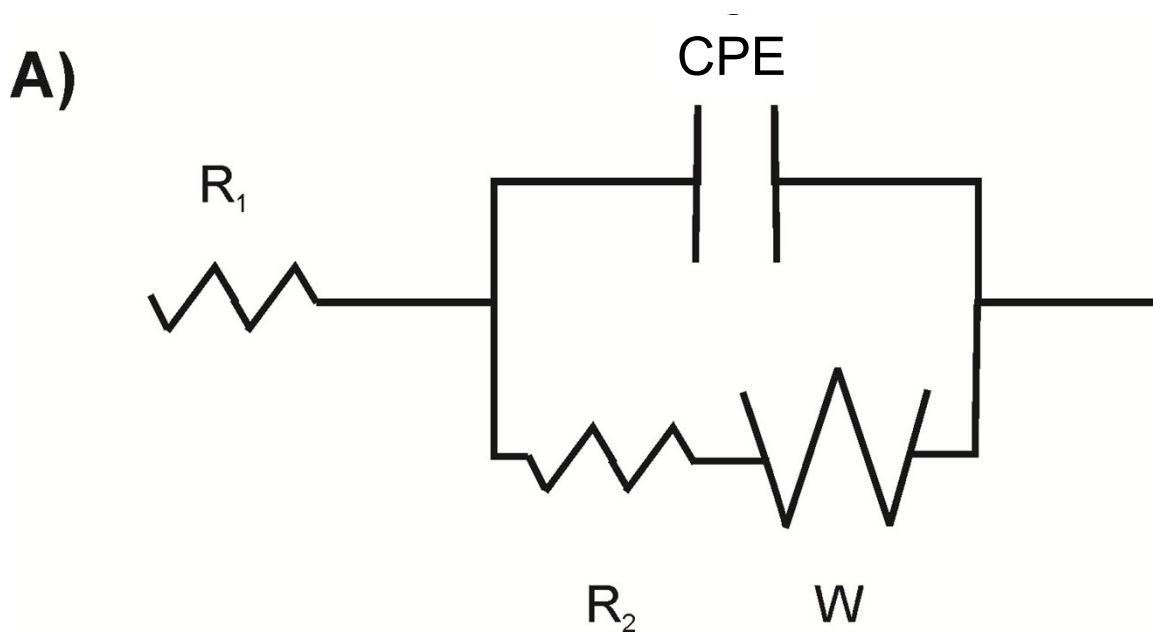
³ IFIMUP-IN and Faculty of Sciences, University of Porto, Rua do Campo Alegre s/n, 4169-007 Porto, Portugal.

<i>A. EIS & Randles-type Equivalent Circuit</i>	2
<i>B. Supplementary Results</i>	3
<i>B.1. Adsorption of Glucose on bare GCE</i>	3
<i>B.2. Response in Pure Buffer</i>	4
<i>B.3. Energy Dispersive Analysis</i>	5
<i>B.4. Reproducibility</i>	6
<i>B.5. Amperometric Calibration</i>	10
<i>B.6. Stability & Durability</i>	11
<i>B.7 Interference Tests</i>	12
<i>C. References</i>	13

* *Corresponding Author Information:* José M. Campiña (PhD), E-mail: jpina@fc.up.pt, Tel: +351 220 402 643

A. EIS & Randles-type Equivalent Circuit

The variation of the Randles circuit [1] used in this work is referred to as R_1QR_2W (see an schematic representation after this paragraph). Instead of the typical capacitor of the Randles circuit, it includes a Constant Phase Element (CPE or Q) which accounts for the topological imperfections of the electrode surface. R_1 is the electrolyte resistance, R_2 is the charge transfer resistance, and W is the Warburg diffusion impedance. When the charge transfer is the rate determining step (for instance, for the GCE/GOx electrode), the Warburg element can be neglected and the system is electrically equivalent to a R_1QR_2 circuit.



B. Supplementary Results

B. 1 Adsorption of Glucose onto bare GCE

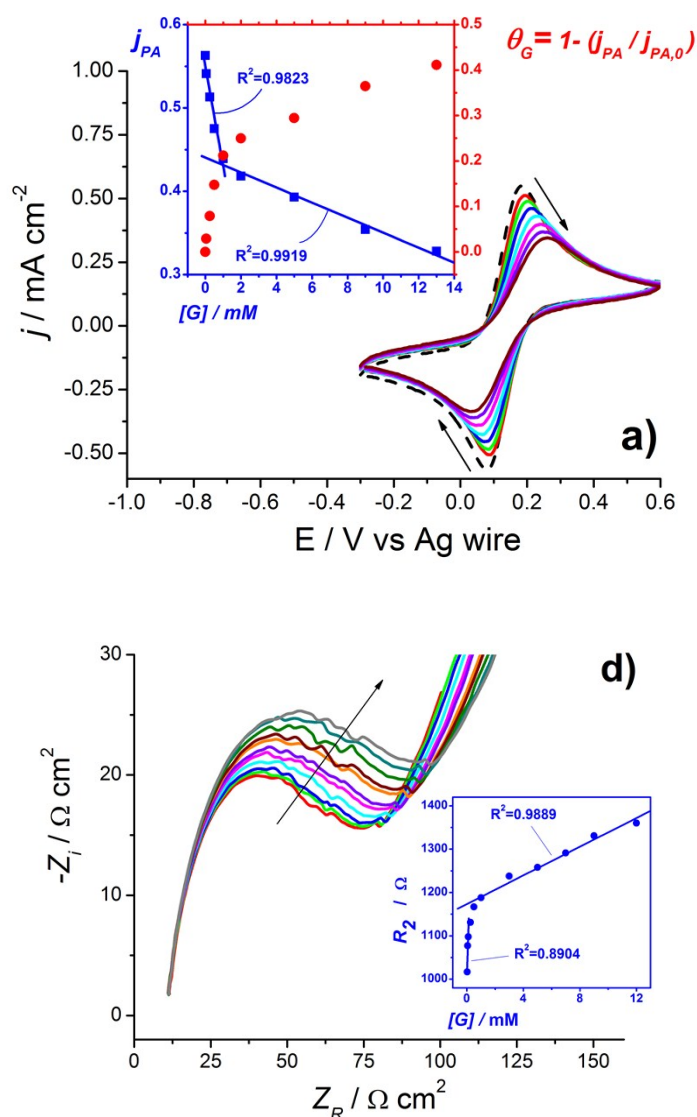


Figure S1. A) CVs for bare GCE in PBS 0.05 M (150 mM NaCl; pH 7.3) + 2 mM $[\text{Fe}(\text{CN})_6]^{3-/4-}$ in the absence (black dashed line) and presence (colored solid lines) of increasing concentrations of D-glucose ($[G]$): 0.05 (red solid line), 0.25 (green), 0.50 (blue), 1.00 (cyan), 5.00 (magenta), 9.00 (violet), and 13.00 mM (wine). The changes in anodic peak currents (j_{PA} ; blue y-axis) and the surface coverage (estimated as $\theta_G = 1 - [j_{PA}/j_{PA,0}]$, with $j_{PA,0}$ being registered in absence of glucose; red y-axis) are plotted versus $[G]$ in the inset. The scan rate was $50 \text{ mV} \cdot \text{s}^{-1}$. **B)** Nyquist plots measured at the half wave potential ($E_{1/2} = +0.15 \text{ V}$) in the range $10^4 - 10^{-1} \text{ Hz}$ (oscillation amplitude: 10 mV). The R_2 values derived from the fittings to the R_1QR_2W circuit are plotted versus $[G]$ in the inset (calibration curves and correlation factors are also included).

B.2. Response of the GOx-Modified Electrodes in Pure Buffer

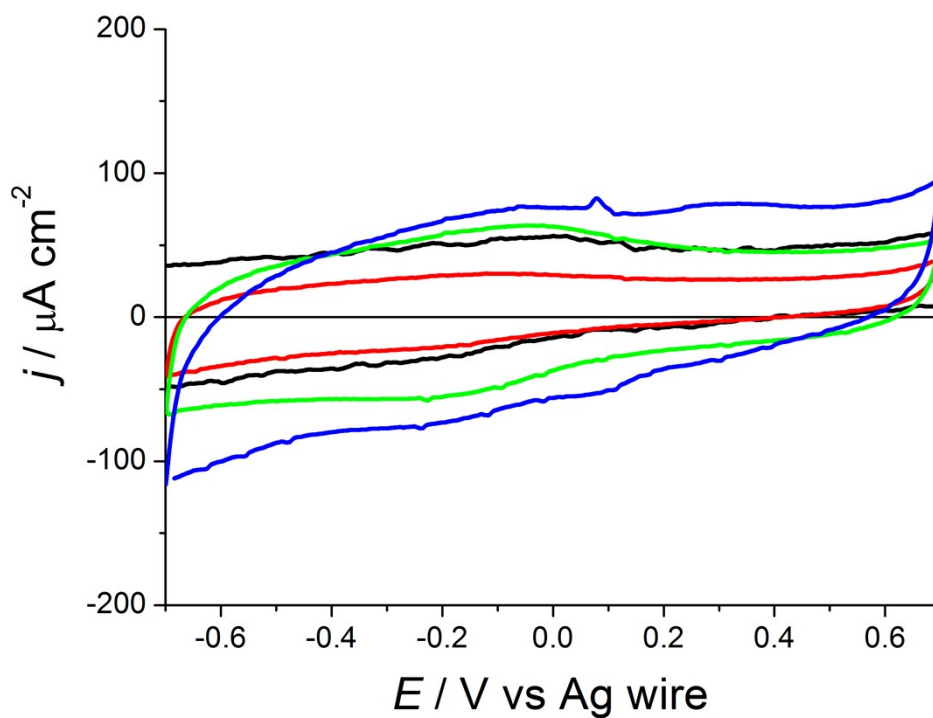


Figure S2. CVs registered for GCE/GOx (red), GCE/Chit95/GOx (green), and GCE/RGO-Ni/Chit95/GOx (blue), in PBS 0.05 M (150 mM NaCl; pH 7.3). The quase-reversible peaks of GOx (which appear at about -0.45 V vs Ag/AgCl [2]) were not found. The voltammogram for a bare GCE (black line) has been included for comparison. The scan rate was $50 \text{ mV} \cdot \text{s}^{-1}$.

B.3. Energy Dispersive Analysis

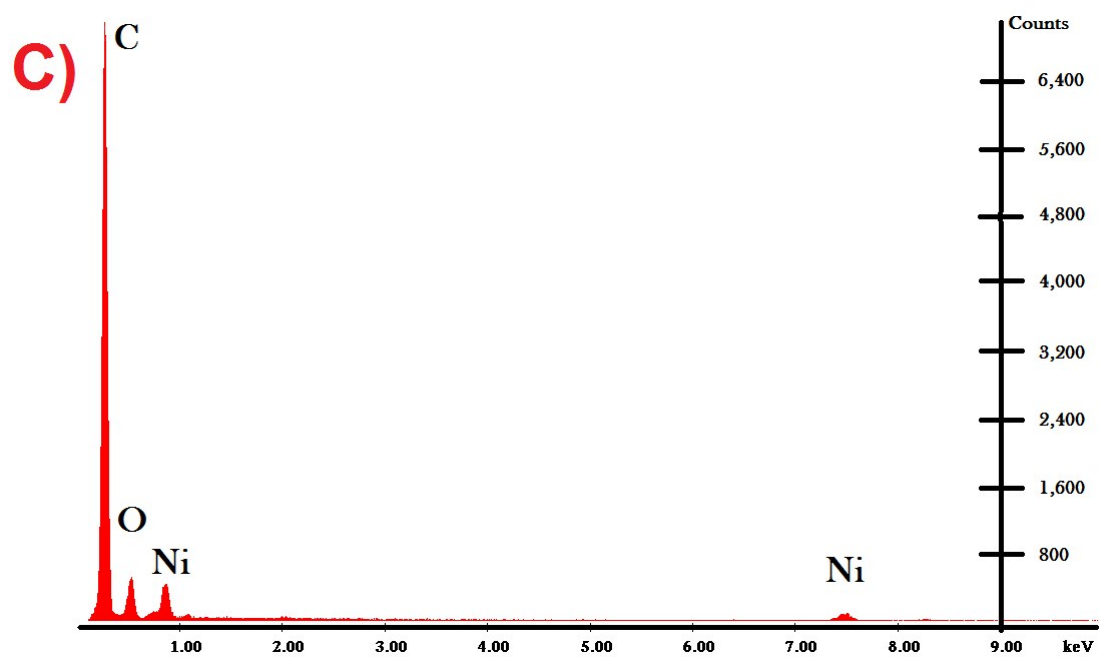
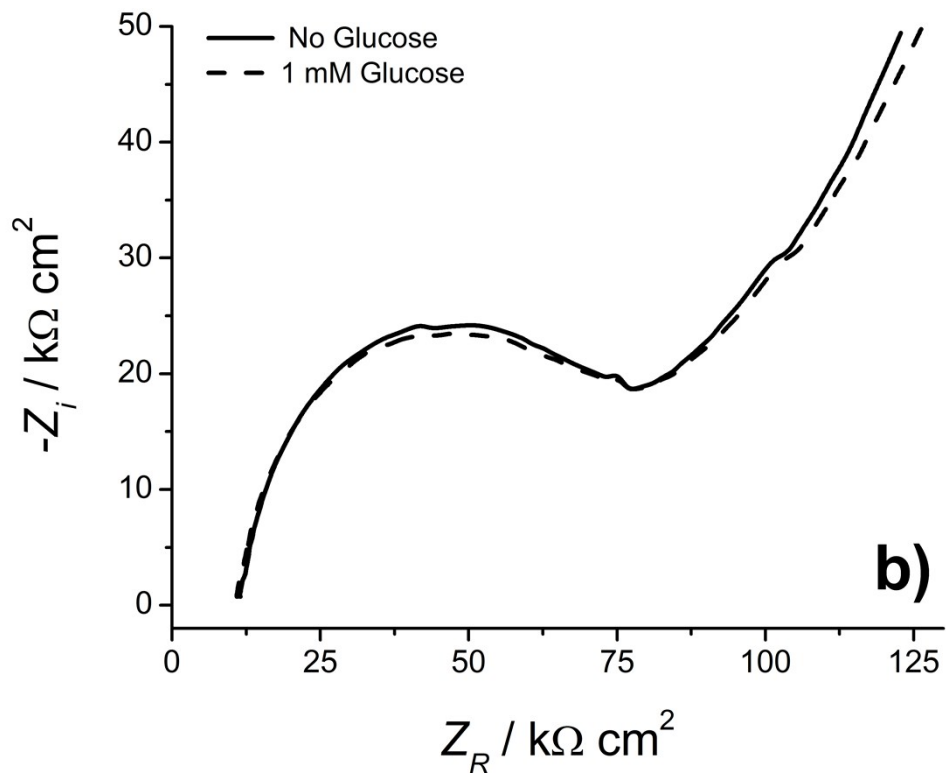
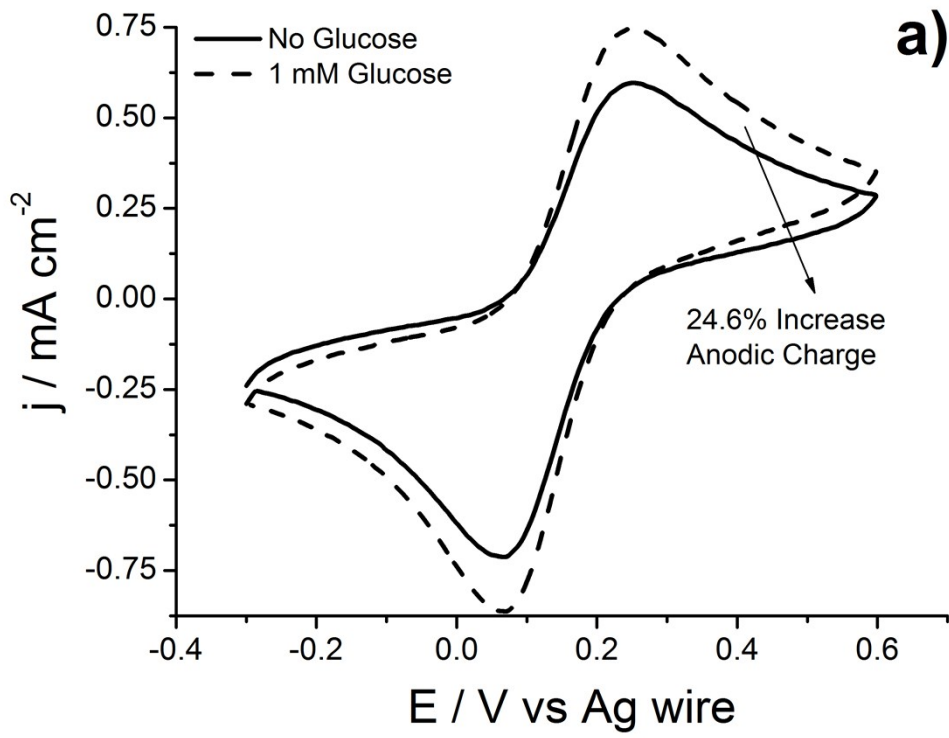


Figure S3. EDS spectrum acquired over the isolated island-type feature isolated in the inset of Fig 4b

B.4. Reproducibility of the Biosensor Response

B.4.1. GCE/rGO-Ni/Chit95/GOx Sample II



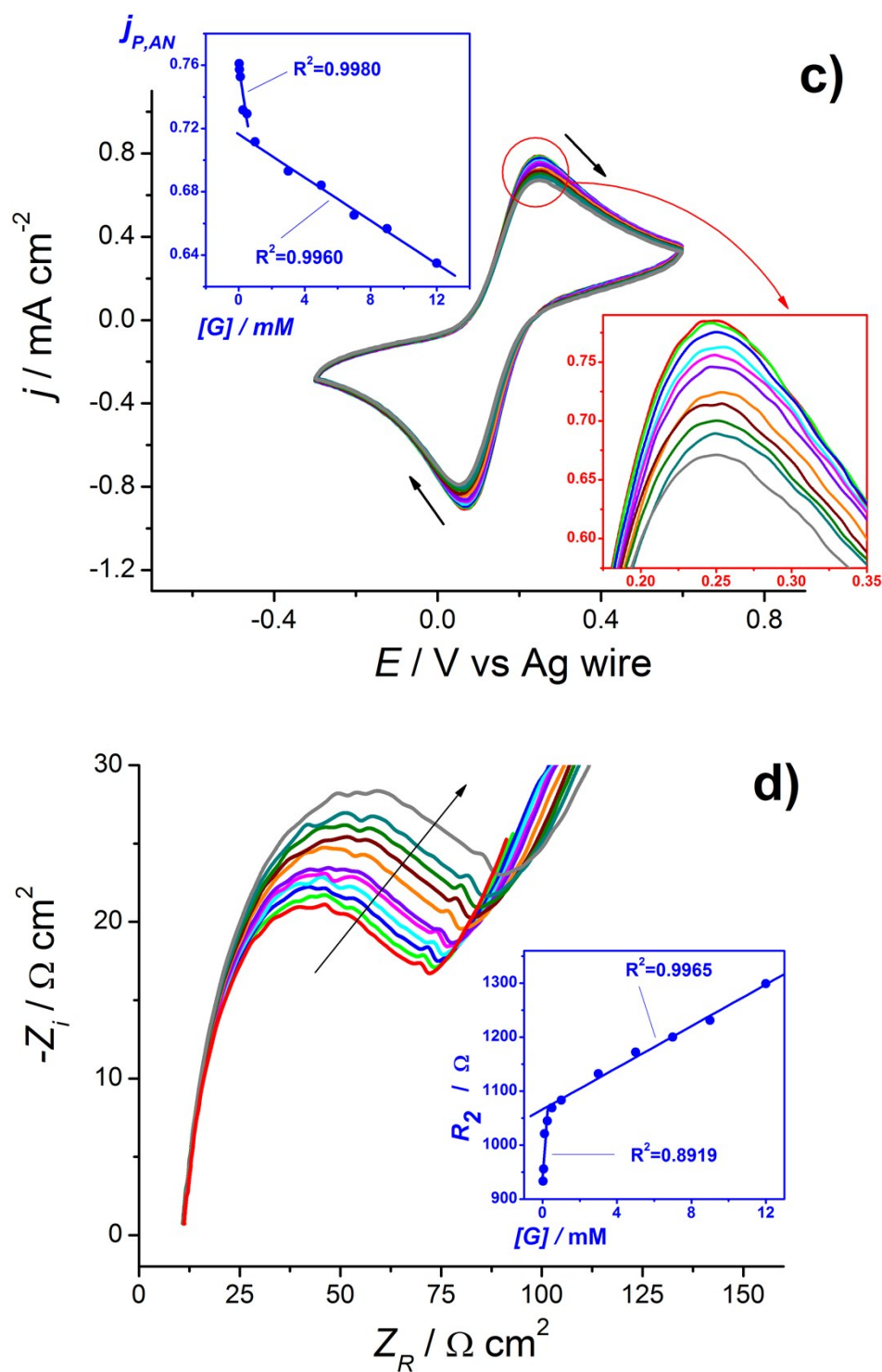
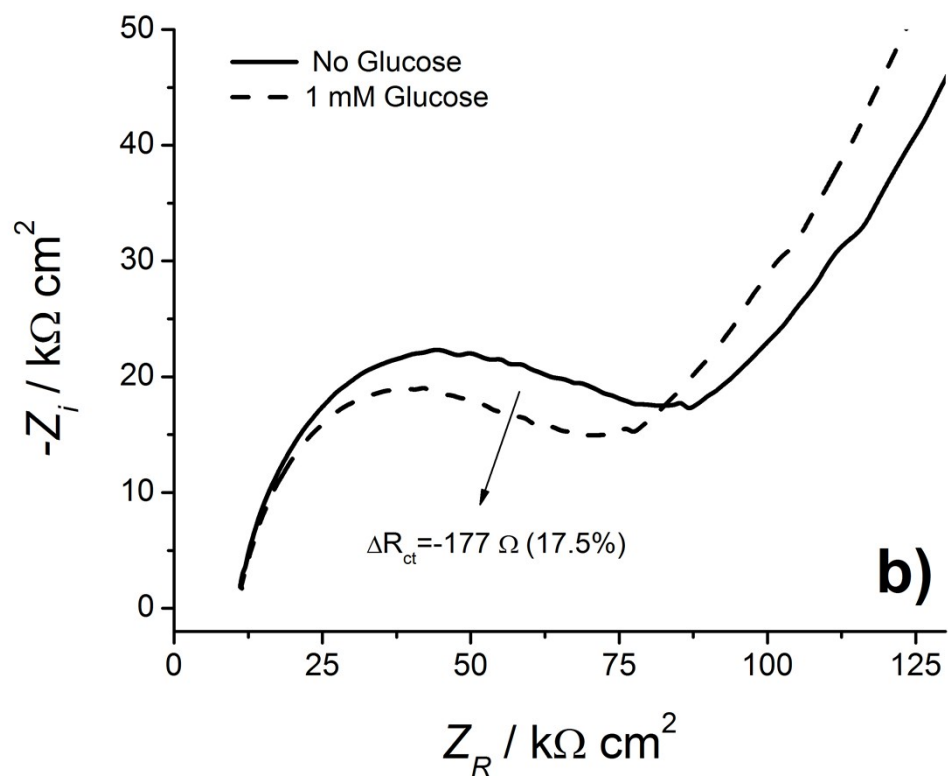
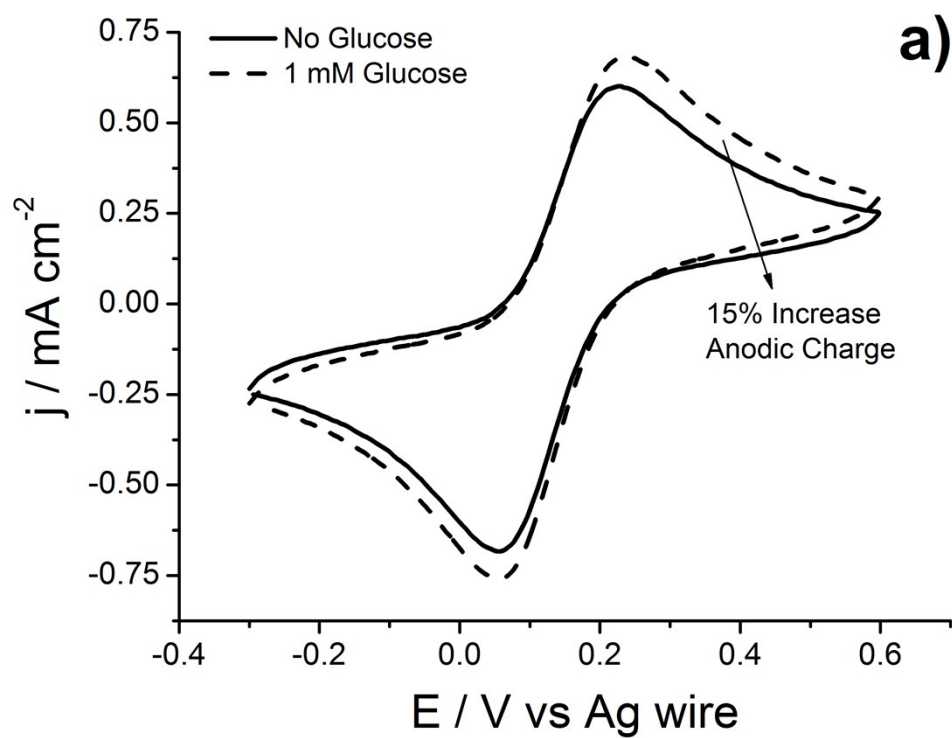


Figure S4. Electrochemical interrogation of GCE/RGO-Ni/Chit95/GOx (sample II) in PBS 0.05 M (150 mM NaCl; pH 7.3) + 2 mM $[\text{Fe}(\text{CN})_6]^{-3/4}$ in the presence of D-glucose. The CVs (a) and Nyquist plots (b) obtained in 1 mM D-Glucose (dashed black lines) are compared with those gathered in its absence (solid lines). (c) CVs and (d) Nyquist plots collected by sweeping $[G]$ from 0.025 to 12 μM (colored solid lines). The anodic peak region is zoomed in the red inset. The j_{PA} and R_2 vs $[G]$ calibration are shown in the blue insets. The scan rate was $50 \text{ mV} \cdot \text{s}^{-1}$ and the impedance spectra taken at +0.15 V (oscillation amplitude: 10 mV).

B.4.2. GCE/rGO-Ni/Chit95/GOx Sample III



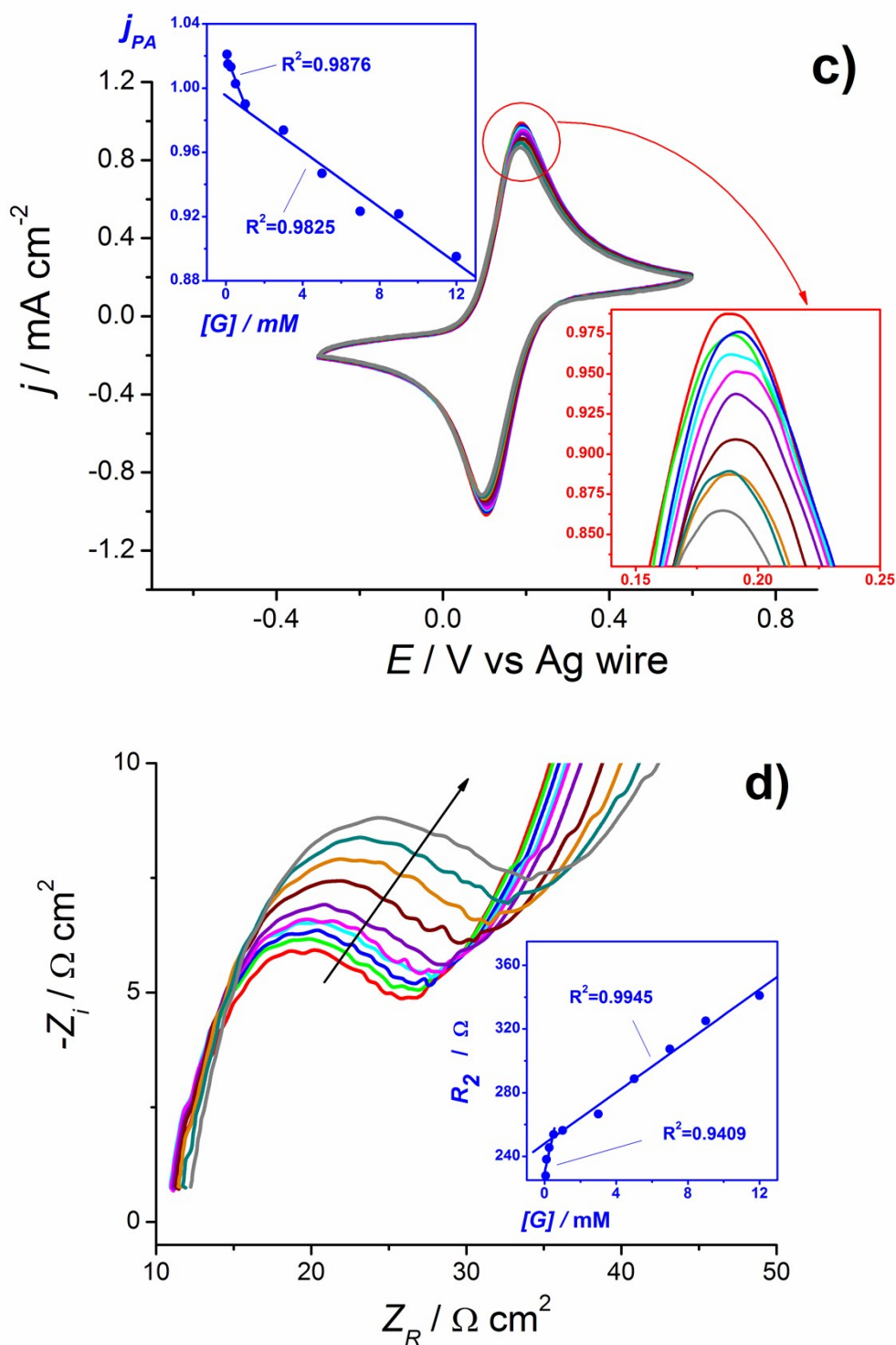


Figure S5. Electrochemical interrogation of GCE/RGO-Ni/Chit95/GOx (sample III) in PBS 0.05 M (150 mM NaCl; pH 7.3) + 2 mM $[\text{Fe}(\text{CN})_6]^{3-/4-}$ in the presence of D-glucose. The CVs (a) and Nyquist plots (b) obtained in 1 mM D-Glucose (dashed black lines) are compared with those gathered in its absence (solid lines). (c) CVs and (d) Nyquist plots collected by sweeping $[G]$ from 0.025 to 12 μM (colored solid lines). The anodic peak region is zoomed in the red inset. The j_{PA} and R_2 vs $[G]$ calibration are shown in the blue insets. The scan rate was $50 \text{ mV} \cdot \text{s}^{-1}$ and the impedance spectra taken at +0.15 V (oscillation amplitude: 10 mV).

B.5. Chronoamperometric Measurements

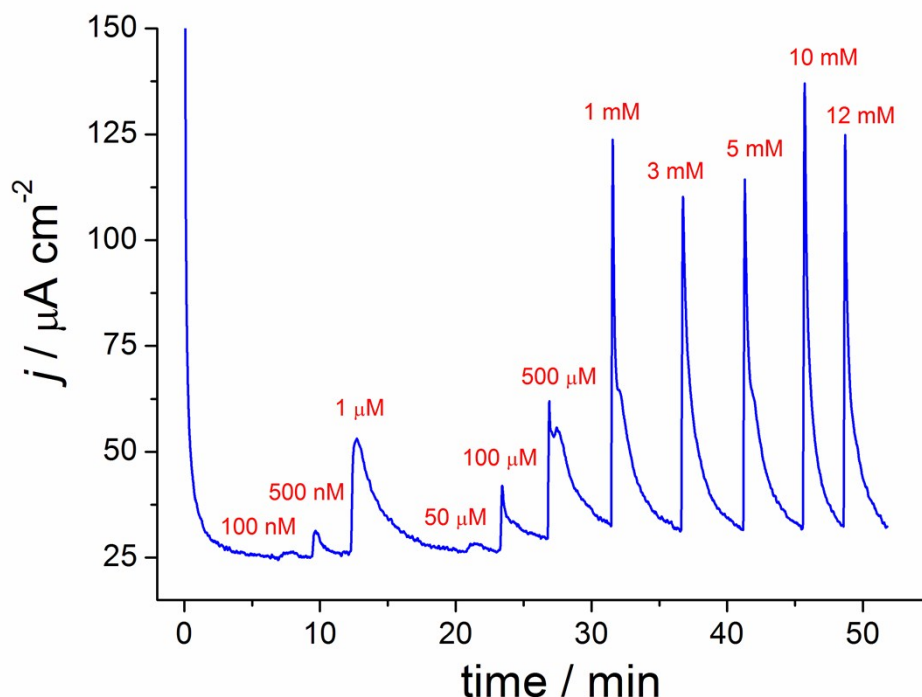


Figure S6. Amperometric interrogation of a GCE/RGO-Ni/Chit95/GOx electrode at the anodic peak potential (+0.20 V vs Ag wire) in PBS 0.05 M (150 mM NaCl; pH 7.3) + 2 mM $[\text{Fe}(\text{CN})_6]^{3-/4-}$. Aliquots of D-glucose were consecutively injected to cover a range of concentration between 25 nM and 12 mM.

To get deeper insights on the responsiveness of the biosensor, the GCE/rGO-Ni/Chit95/GOx electrode was potentiostatically interrogated within an enlarged range of $[G]$ (Fig S6). At the anodic peak potential, the $[\text{Fe}(\text{CN})_6]^{4-}$ probe is continuously oxidized to $[\text{Fe}(\text{CN})_6]^{3-}$. Under this approach the probes are solution species with finite concentration (2 mM) vs the bulky surface MNPs/SNPs used in most non-enzymatic sensors. Hence, the concentration of $[\text{Fe}(\text{CN})_6]^{4-}$ is depleted causing the current to fall until a diffusion limited current density is reached ($\approx 25 \mu\text{A}\cdot\text{cm}^{-2}$). When glucose is injected, the activity of GOx regenerates $[\text{Fe}(\text{CN})_6]^{4-}$ and its re-oxidation generates the peaks. The regenerated probe is readily reoxidized so that the current follows a fast decline and no plateau is achieved. For this reason, we have not used these data to build a calibration curve. However, they demonstrate the high responsiveness of the biosensor even for $[G]$ as low as 0.1 μM glucose.

B.6. Stability & Durability

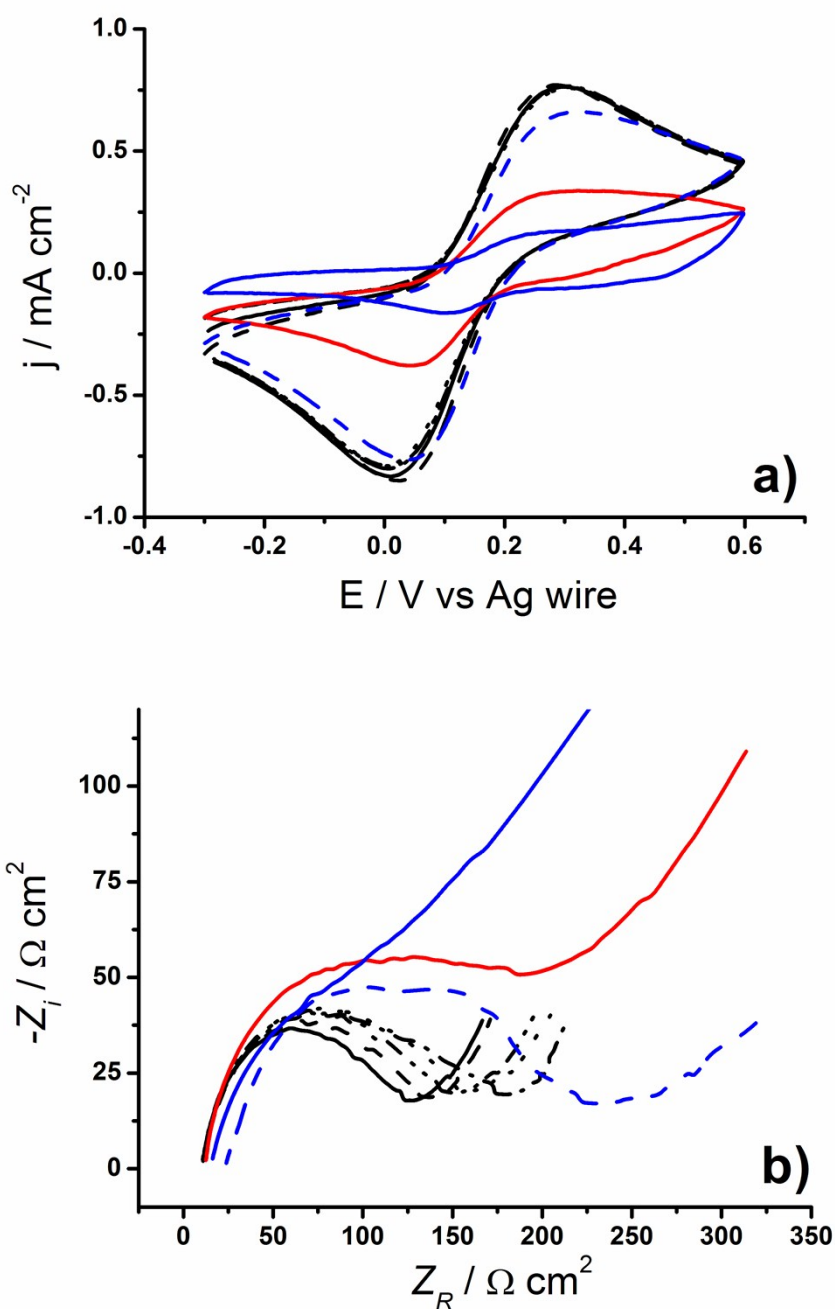


Figure S7. CVs (a) and Nyquist plots (b) recorded for a GCE/rGO-Ni/Chit95/GOx in PBS 0.05 M (150 mM NaCl; pH 7.3) + 2 mM $[\text{Fe}(\text{CN})_6]^{3-/4-}$ + 1 mM D-glucose. The first five CVs/Nyquist plots consecutively registered for this electrode, are presented as black curves: 1st (solid), 2nd (dashed), 3rd (dash dotted), 4th (dash dot dotted), and 5th (dotted). From the additional 95 voltammograms and impedance spectra registered, only the curves for the 100th are shown (solid red). The CVs for other freshly prepared electrodes stored for three weeks at 4°C under either dry (blue solid curves) or wet conditions (blue dashed curves) are also included. The scan rate was $50 \text{ mV} \cdot \text{s}^{-1}$ and the impedance spectra were taken at +0.15 V (oscillation amplitude: 10 mV).

B. 7. Interference Tests

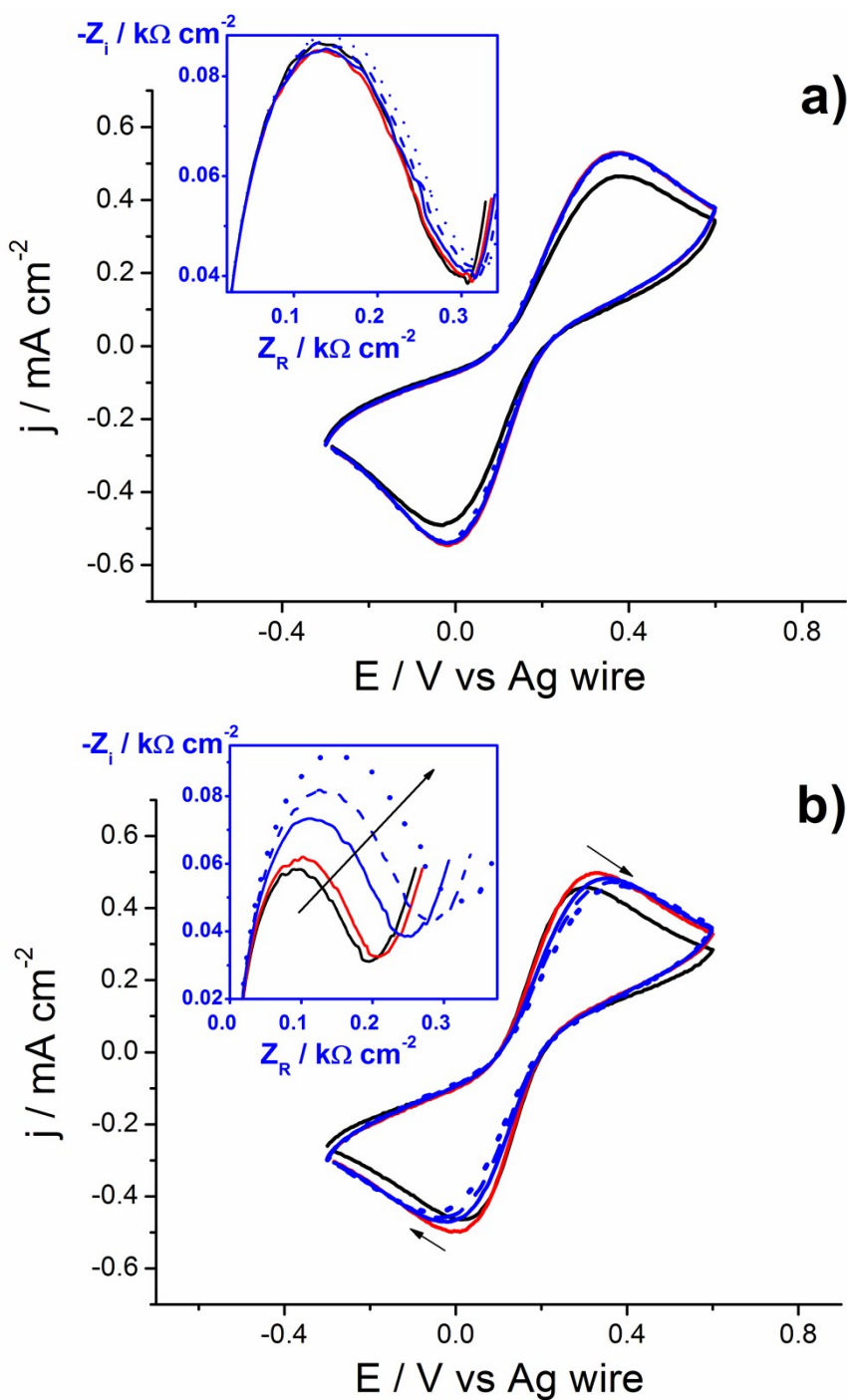


Figure S8. CVs Interference tests in presence of ascorbic acid (AA) and uric acid (UA) (blue lines). **(a)** CVs registered for the GCE/rGO-Ni/Chit95/GOx biosensor in PBS 0.05 M (pH 7.3) + 2 mM $\text{Fe}(\text{CN})_6^{3-/4-}$ + 1 mM D-glucose (red line) after addition of AA to final concentrations of 50 (solid), 75 (dashed), and 100 μM (dotted). The voltammetric profile obtained in absence of glucose is also included for comparison (black line). The impedance spectra obtained under identical conditions are included in the blue inset. **(b)** Analogous experiments were carried out by addition of UA (same line styles and color keys apply). The scan rate was $50 \text{ mV} \cdot \text{s}^{-1}$ in all cases.

C. References

- [1] J. E. B. Randles, Kinetics of Rapid Electrode Reactions, *Discuss. Faraday Soc.* **1947**, 1, 11-19.
- [2] G. Bharath, R. Madhu, S-M. Chen, V. Veermani, A. Balamurugan, D. Mangalaraj, N. Ponpandian, Enzymatic Electrochemical Glucose Biosensors by Mesoporous 1D Hydroxyapatite-on-2D Reduced Graphene Oxide, *J. Mater. Chem. B* **2015**, 3, 1360-1370